Geomechanics and Engineering, *Vol. 26, No. 5 (2021) 477-487*
https://doi.org/10.12989/gae.2021.26.5.477

Effect of heat treatment and bedding orientation on the tensile properties of bedded sandstone

Xinshuai Shi[1,2,3], Yujing Jiang[1,3], Hongwen Jing[*2], Yuanchao Zhang[3], Yuan Gao[2], Zhenlong Zhao[2] and Qian Yin[2]

[1]*College of Energy and Mining Engineering, Shandong University of Science and Technology, Qingdao 266590, PR China*
[2]*State Key Laboratory for Geomechanics and Deep Underground Engineering, China University of Mining and Technology, Xuzhou 221116, PR China*
[3]*Graduate School of Engineering, Nagasaki University, 1-14 Bunkyo, Nagasaki 852-8521, Japan*

(Received June 2, 2020, Revised May 21, 2021, Accepted September 7, 2021)

Abstract. The effect of heat treatment and the bedding orientation on the tensile properties, the central strain and failure patterns of bedded sandstone specimens were studied under Brazilian test conditions. The laboratory test results show that the tensile strength decreases with increasing bedding orientation at different temperatures, which indicates the bedded sandstone possesses prominent anisotropy in tensile strength. The anisotropy coefficient first increases and then decreases with the increasing temperature. For all temperatures, both V-strain and S-strain present a decreasing trend with increasing bedding orientation. However, for all bedding orientations, the S-strain first increases and then decreases, but V-strain continues to increase with increasing temperature. Furthermore, the failure patterns of the failed specimens are generally classified into three categories: central across the bedding planes (CF), fracture along the bedding planes (LA) and the mixed fracture patterns of the two. Finally, the evolution of the internal structure of the disk specimens after different heat treatments was investigated by SEM tests. The specimen profile looks smoother and denser at 400℃ and 600℃, but at 800℃ and 1000℃, the internal structure of the specimen is sharply deteriorated by thermal reactions.

Keywords: bedded sandstone; bedding orientation; failure patterns; heat treatment; tensile properties

1. Introduction

There is growing interest in studying the thermal properties of rocks at high temperature or after heating treatments in recent years. The rocks were involved in high-temperature circumstances, such as the disposal of highly radioactive nuclear waste, exploitation of the geothermal resource, underground coal gasification, and post-disaster reconstruction of buildings after exposure to fire (Becattini *et al.* 2017, Cheng *et al.* 2020, Liu *et al.* 2021, Tomac and Sauter 2018, Wang *et al.* 2020). The physical and mechanical properties of rock, including the density, wave velocity, strength and elastic modulus, will undergo noticeable variation after high-temperature treatment.

Extensive studies have been conducted to understand the effect of temperature on the rock's physical and mechanical properties. The tensile performance was a very sensitive parameter for the stability of geological engineering structures (Komurlu *et al.* 2016, Zhou *et al.* 2018, Wang *et al.* 2019, Xue *et al.* 2020). The rocks are more prone to fail under tensile loading because the tensile properties are much weaker than the compressive and shear properties. Thus, the research concerning the correlation of heat treatment with the tensile strength of the rock material has attracted considerable attention. Sirdesai *et al.* (2017) investigated the effect of temperature and thermal durations on the tensile strength of red sandstone. They pointed out that the primary reason for the change of tensile strength can be attributed to the mineral expansion within the rock samples after high-temperature treatment, and the thermal durations also had a significant impact on the tensile strength. Lü *et al.* (2017) reported that the loss of water and minerals and the effect of thermal stress resulted in the change of the tensile properties of sandstone. They divided the variation of tensile strength with temperature into four phases: from room temperature to 300 °C, 300 ~ 600 °C, 600 ~ 800 °C, 800 ~ 900 °C. Yin *et al.* (2015) studied the relationship between the tensile strength and elevated temperatures by using an MTS hydraulic servo-control testing system and a modified split Hopkinson pressure bar (SHPB) system. The static tensile strength showed a decreasing trend while the dynamic tensile strength first increases and then decreases with increasing temperature.

The above studies mainly focused on relatively homogeneous rocks. However, many natural rocks usually contain some well-defined fabric elements, such as bedding planes, stratification, foliation, cleavage, or jointing, leading to pronounced anisotropy in the physical and mechanical properties (Roy and Singh 2016, Tavallali and Vervoort 2010). The anisotropic properties also play a vital role in rock mass behaviours. Many experimental studies have been conducted to reveal the anisotropic behaviours in the tensile strength of various anisotropic rocks, e.g., Nezhad *et*

*Corresponding author, Professor
E-mail: hongwenjingcumt@126.com

ISSN: 2005-307X (Print), 2092-6219 (Online)

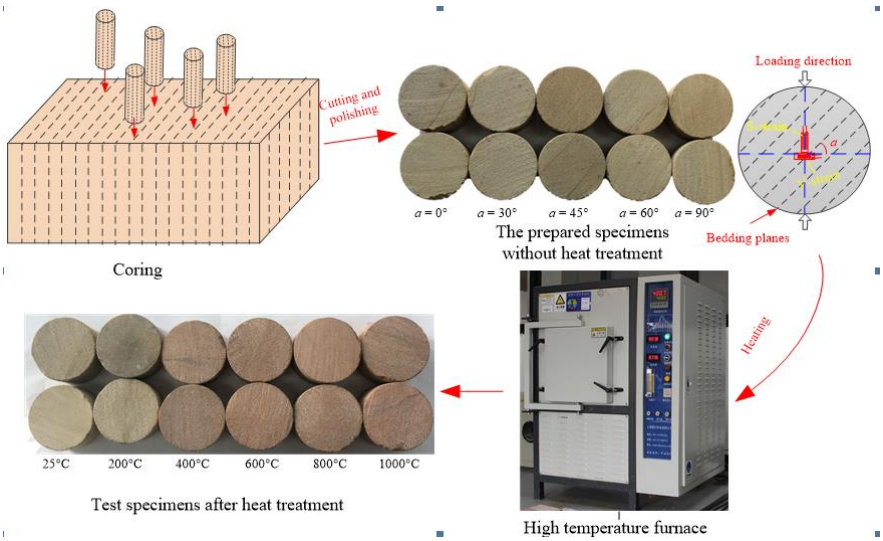

Fig. 1 Preparation of the test specimens

al. (2016), Keneti and Wong (2010) as well as Mokhtari *et al.* (2014) on shale; Nasseri *et al.* (2003) on schists; Gholami and Rasouli (2014) and Debecker and Vervoort (2009) on slate; Tavallali and Vervoort (2010) and Khanlari *et al.* (2015) on laminated sandstone. A review of the aforementioned experimental investigations indicated that the presence of the bedding structures had a significant effect on the tensile strength and failure patterns of the anisotropic rocks. Khanlari *et al.* (2015) evaluated the compressive strength, Brazilian tensile strength and failure patterns of the layered sandstone with different inclination angles. They found that the anisotropy ratio of the compressive was lower than that of the tensile strength, and the failure patterns were summarized as parallel to the lamination (PL), across the lamination (AL) and mix of failure patterns of the two under Brazilian test. Yang *et al.* (2019) reported that the tensile strength of shale decreased gradually with respect to bedding inclination, and the anisotropic behaviours were depended on the bedding inclination and interlayer bonding force. Until now, there were limited studies considering the effect of heat treatment on the tensile strength of layered rocks. The interaction mechanism between bedding orientation and high temperature on the tensile behaviours of anisotropic rocks remains unclear.

Here, the tensile properties of the bedded sandstone specimens with different bedding orientations are measured under six different heat-treatment temperatures ranging from 25 °C to 1000 °C. First, the effect of the bedding orientation and heat treatment on the tensile properties of bedded sandstone were systematically analyzed. Then, the strain observation system was applied to investigate the central strain evolutions during the failure process. Furthermore, the ultimate failure patterns for the failed disk specimens were classified. Finally, the microscopic mechanism of heat treatment on the tensile properties of the tested sandstone was revealed by using scanning electron microscopy (SEM) analysis. The experimental results provide a significant reference for understanding the combined effect of bedding and temperature on the tensile properties of anisotropic rocks, further ensuring the safety and security of underground engineering structure.

2. Experimental material and testing procedures

2.1 Specimens preparation

The specimens were firstly drilled from the same block of sandstone materials using a 50 mm diameter drill bit. The direction of coring is parallel to the bedding planes. Then, the core specimens were cut into several standardized disc-shaped specimens with a thickness-to-diameter ratio of 0.5 (ASTM D3967–08 2008). After the prepared specimens were dried at room temperature for the next 48 h, the size (diameter and thickness) and mass were recorded by taking an average value of three readings for each of the cases. Then, the specimens were heated to the designed 200, 400, 600, 800 and 1000 °C by using GWD-02A High-Temperature Furnace, and one set was tested directly at room temperature. The heating rate of the furnace was set as 5 °C/min to avoid thermal shock. After reaching the required temperature, the specimens were treated at a constant temperature for two hours, and then rock specimens were cooled to room temperature in the furnace naturally. The surface color of sandstone samples changes from initial ochre to reddish-brown after heat treatment. The test specimens preparation process is shown in Fig. 1. For each combination of bedding orientation and temperature, three specimens were prepared to get a representative value, and a total of 90 specimens are prepared for the present research.

X-ray fluorescence (XRF) and X-ray diffraction (XRD) analysis were used to identify the major elements and the mineral compositions of the tested sandstone, and the results are shown in Fig. 2. The XRF test results show that the highest element of the original bedded sandstone is SiO_2 with an average value of 73.26%, which is followed by Al_2O_3 with a mean level of 11.22%, and small amounts of Fe_2O_3, K_2O, CaO, MgO, and Na_2O can also be observed.

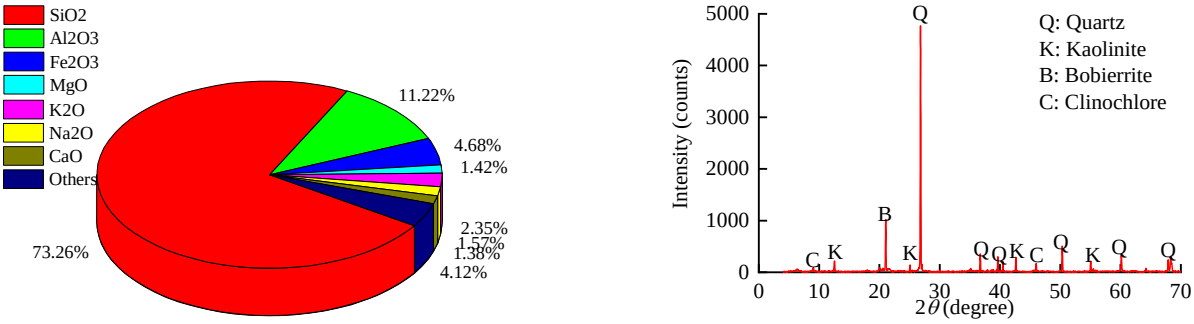

(a) XRF (b) XRD

Fig. 2 Main chemical and mineral composition of the bedded sandstone

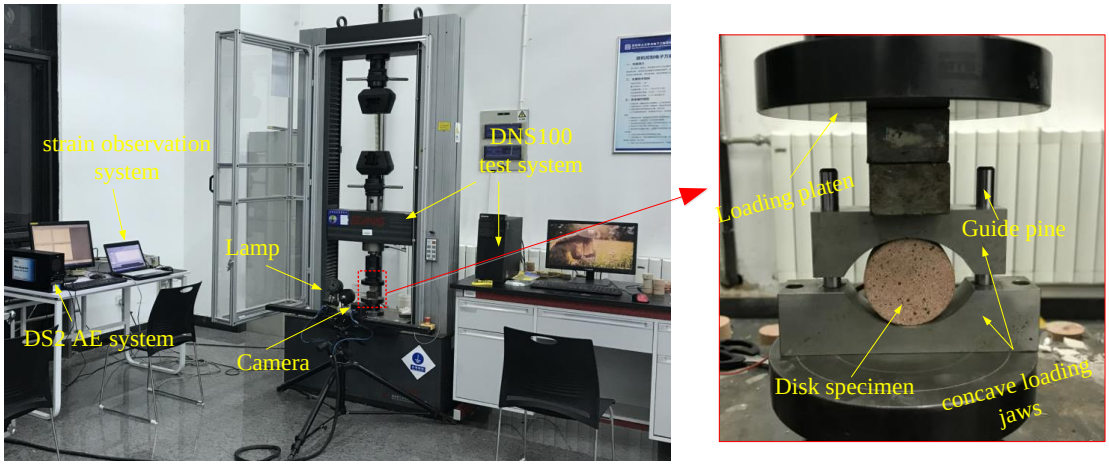

Fig. 3 Test system configuration diagram

The XRD test results show that the main minerals were identified to be quartz, kaolinite, bobierrite and clinochlore.

2.2 Experimental equipment and testing procedures

The Brazilian test is a simple indirect testing method to measure the tensile strength of the rock. In this experiment, the tested disk specimen is first placing in the concave loading jaws, as shown in Fig. 3. Then this configuration with the specimen is placed in the DNS100 electronic universal testing machine. The loading system can be controlled by force or displacement loading modes with a maximum load capacity of 300 kN. During the loading process, the loading rate is set to 0.1mm/min to avoid the effect of impact. The indirect tensile strength of the rock is measured by the Brazilian split test, which can be calculated as follows:

$$\sigma_t = \frac{2P}{\pi Dt} \tag{1}$$

where P is the maximum failure load applied to the disk specimen (kN), D and t are the diameter and thickness of the tested specimen (mm). It should be noted that the above equation may not be suitable for the case of the isotropic rock material. But the formula is only used for the purpose of the comparison herein (Tavallali *et al.*2010, Roy *et al.*2016, Yang *et al.* 2019).

For each of the temperatures, the tensile properties of the bedded sandstone are measured at five different bedding orientations. The bedding orientation (a) is defined as the angle between the bedding plane and horizontal direction, as shown in Fig. 1. During the compression process, central strain in two directions is recorded by the strain gauges; one is perpendicular (S-strain) and another is parallel (V-strain) to the loading direction.

3. Results and discussion

3.1 Tensile strength

Fig. 4 shows the variation of Brazilian tensile strength (BTS) with the inclination angles for the specimens after different heat treatments. For all temperatures, the tensile strength of the bedded sandstone specimens systematically decreases with increasing bedding orientation, approximating a negative linear variation. The maximum value usually occurs at α=0°, and the minimum value usually occurs at α=90°. From these observations, it is interpreted that the existence of the weak bedding planes has a profound effect on the tensile strength properties of the bedded sandstone specimens, even after thermal treatment. The bedded sandstone possesses obviously anisotropic characteristics in tensile strength at different

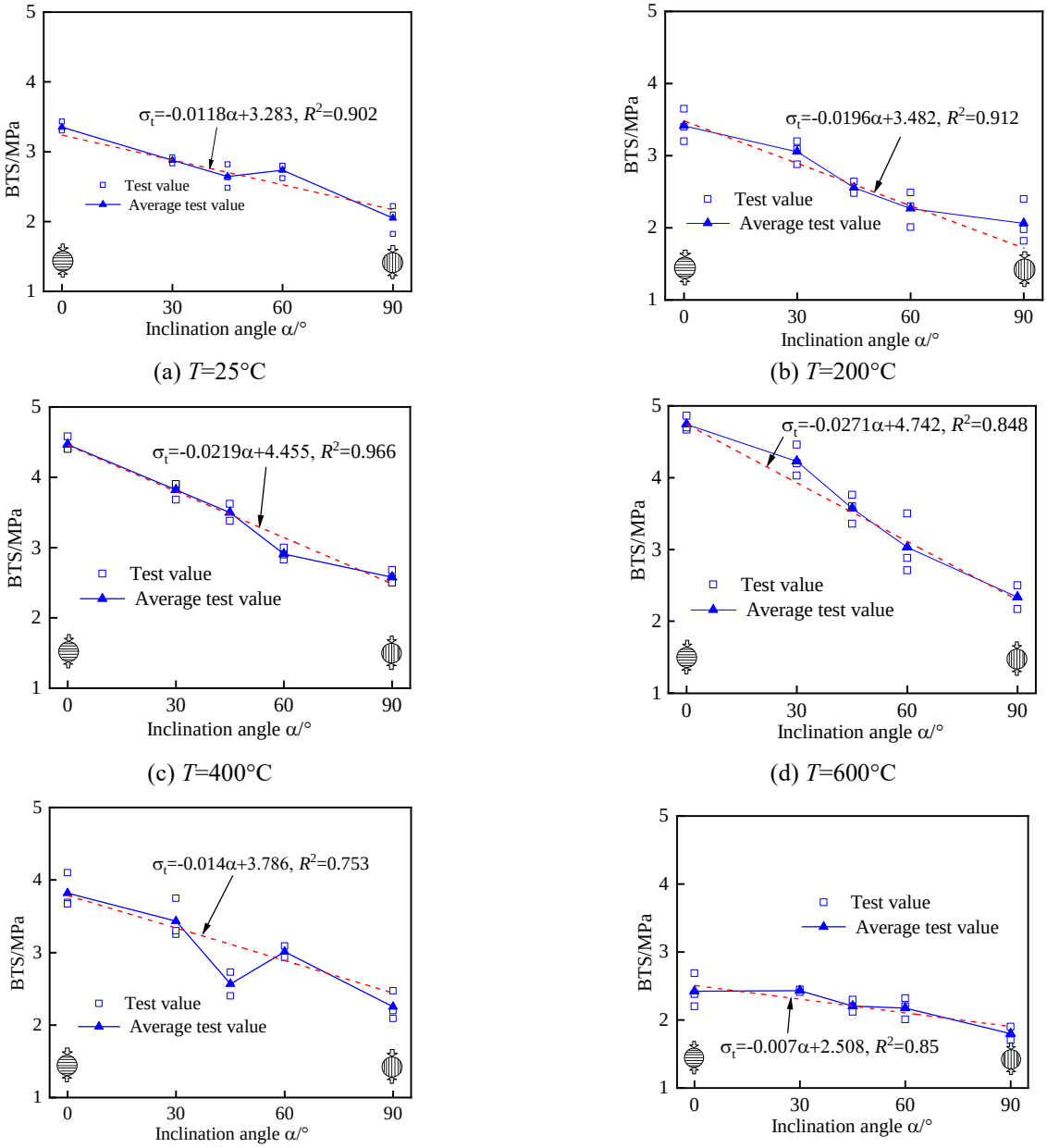

Fig. 4 Variation of BTS with the inclination angle

heat-treatment temperatures. Here, we define an anisotropy coefficient to quantitatively evaluate the tensile strength anisotropy of bedded sandstone (Chong *et al.* 2017), which can be calculated as follows:

$$R_t = \frac{\sigma_{t(max)}}{\sigma_{t(min)}} \quad (1)$$

where R_t is the anisotropy coefficient, $\sigma_{t(max)}$ and $\sigma_{t(min)}$ are the maximum and minimum average values of the BTS under different temperatures, respectively.

The R_t of the test specimens at different temperatures can be calculated by Eq. (2) and is shown in Fig. 5. From Fig. 5, it can be observed that the high-temperature treatment has a visible effect on the anisotropy degree of tensile strength. R_t presents a changing trend of first increase and then decrease with increasing T. Before T=600°C, the anisotropy degree is improved, R_t increases from 1.57 at room temperature to 1.76 at T=600°C. As T further increases to 800°C and 1000°C, the anisotropy degree is weakened. R_t decreases to 1.60 at T=800°C and 1.51 at T=1000°C. The anisotropy coefficient at T=1000°C is even slightly smaller than that at room temperature. All of these may be attributed to the high temperature playing a different role in changing the tensile properties of sandstone with different bedding orientations.

To further analyze the influence of high temperature on the tensile strength properties of bedded sandstone. Fig. 6 shows the evolution of BTS with increasing temperature under a constant bedding orientation. The tensile strength

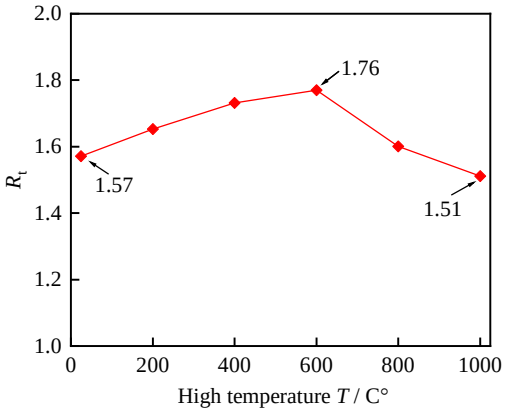

Fig. 5 Variation of R_t with T

Table 1 Variation rate of tensile properties of bedded sandstone after thermal treatment

Bedding orientation	Average BTS			Variation rate	
	T= 25°C	T= 600°C	T= 1000°C	Inceasing stage	Decreasing stage
0°	3.35	4.74	2.42	41.49%	-48.94%
30°	2.87	4.23	2.43	47.38%	-42.55%
45°	2.64	3.57	2.21	35.22%	-38.09%
60°	2.73	3.03	2.17	10.98%	-28.38%
90°	2.05	2.33	1.80	13.66%	-22.74%

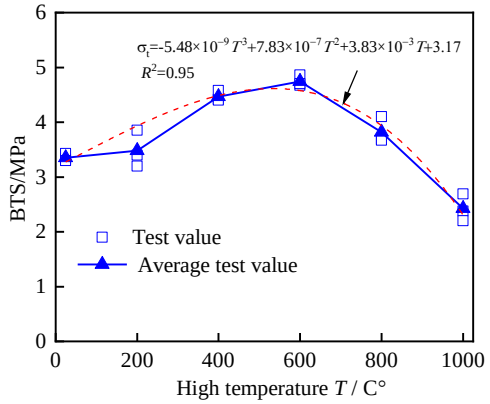

(a) α= 0°

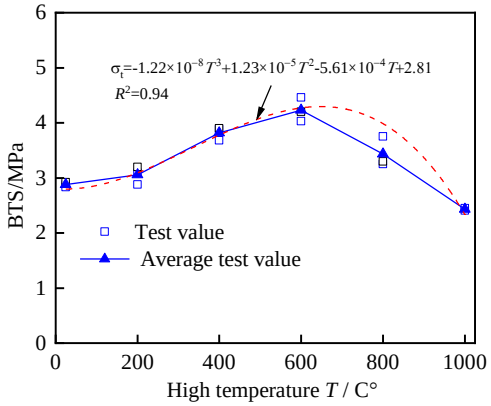

(b) α= 30°

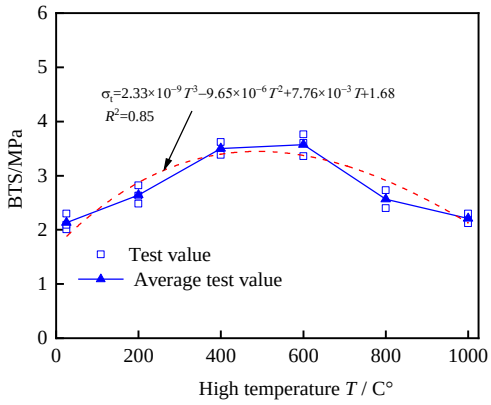

(c) α= 45°

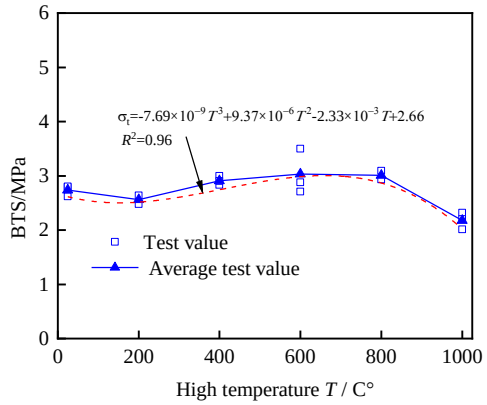

(d) α= 60°

Fig. 6 Variation of BTS with T

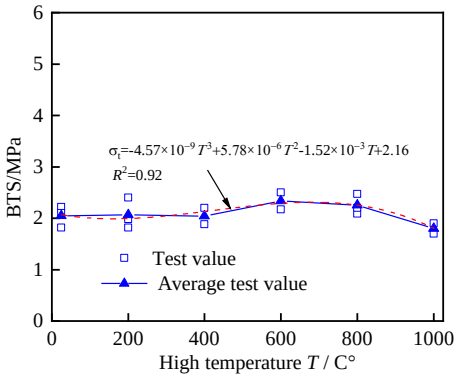

(e) α= 90°

Fig. 6 Continued

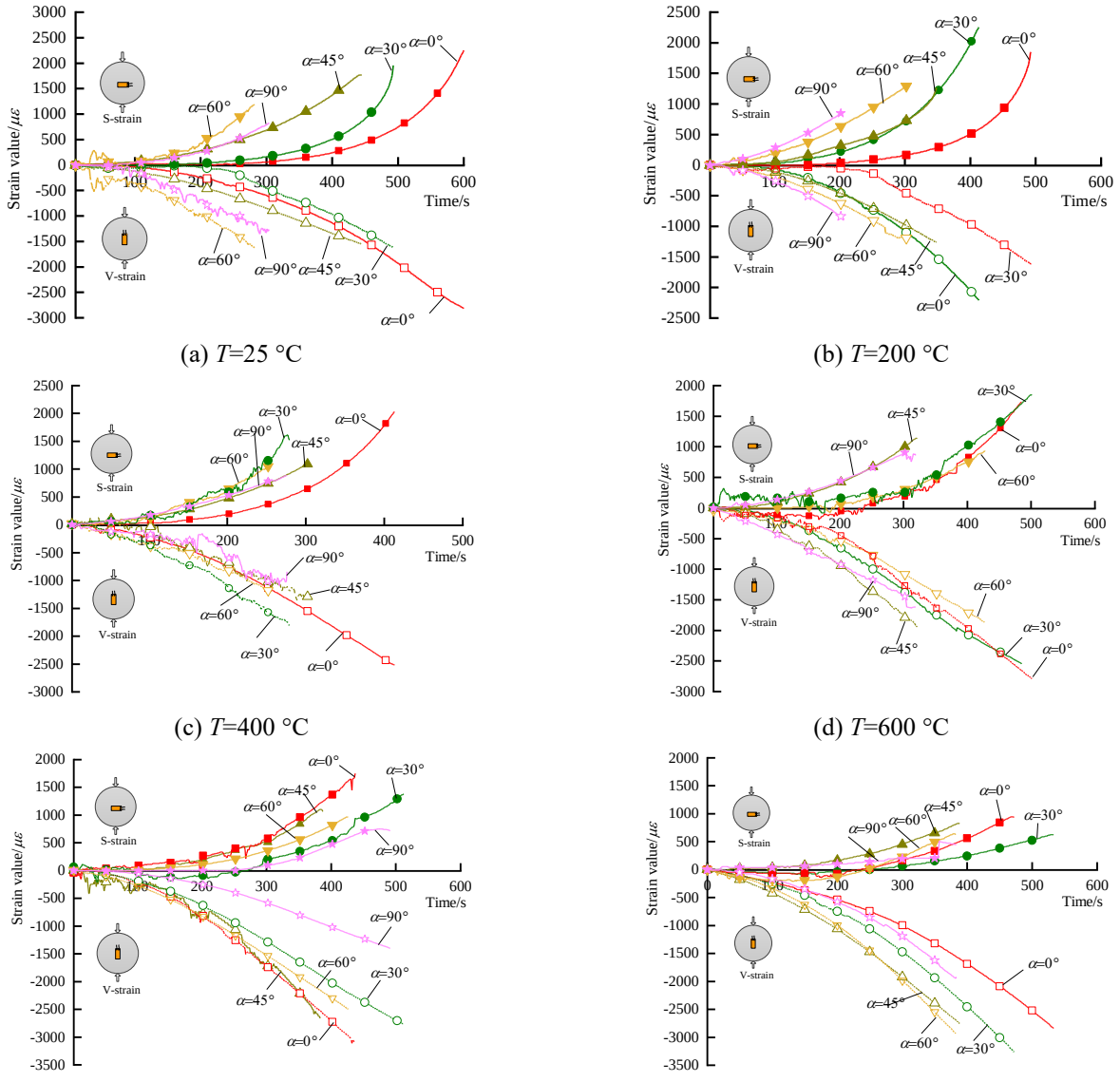

(a) T=25 °C (b) T=200 °C

(c) T=400 °C (d) T=600 °C

(e) T=800 °C (f) T=1000 °C

Fig. 7 Central strain evolution of bedded sandstone specimens with the varying inclination angle

presents a similar non-linearly change with increasing treatment temperature for the specimens at different bedding orientations. From room temperature to 600°C, the tensile strength increases gradually. When the temperature increases from 600°C to 1000°C, the tensile strength presents a decreasing trend. It can also be seen that their

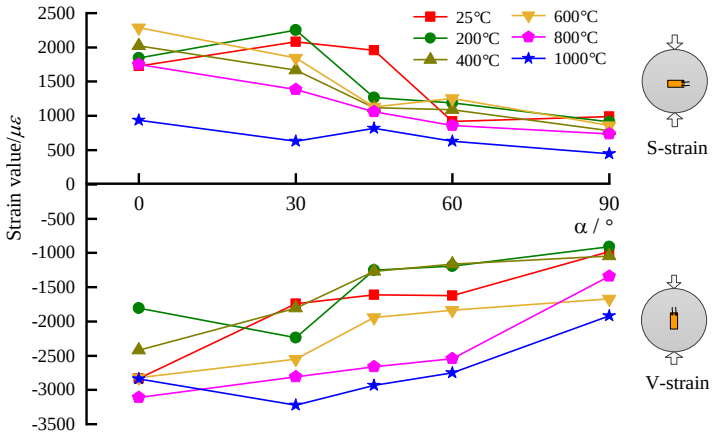

Fig. 8 Variation of failure strain with bedding orientation under different temperatures

tensile strength appears the different variation rates in both the increasing stage and decreasing stage for the specimens with different bedding orientations. For the specimens with 0°, 30° and 45° bedding orientation, when the temperature increases from 25 °C to 600 °C, the peak tensile strength increases by 41.49%, 47.38% and 35.22%, respectively. As the temperature further increases from 600 °C to 1000 °C, the peak tensile strength decrease rates are 48.94%, 42.55% and 38.09%. However, for the specimens with bedding orientation of 60° and 90°, the peak tensile strength increases by only 10.98% and 13.66% in the range of 25 °C~600 °C. When the temperature increases from 600 °C to 1000 °C, the peak tensile strength decreases by 28.38% and 22.74%. It is evident from the above values that as the specimens are treated at increasingly higher temperatures, the peak tensile strength change obviously at lower bedding orientation (α=0°, 30° and 45°) than that at higher bedding orientation (α=60° and 90°). The average tensile strength values and variation rate are shown in Table 1.

3.2 Central strain analysis

To investigate the effect of bedding orientation and temperature on the central strain features of bedded sandstone specimens, strain evolution in two directions, e.g., perpendicular (S-strain) and parallel (V-strain) to the loading direction, were recorded simultaneously by the strain gauges. Fig. 7 shows the V-strain and S-strain evolution with loading time for bedded sandstone with varying inclination angles at different temperatures. The positive and negative values in the figure represent tension and compression strain, respectively. The strain gauges usually break as the specimens fail, and the strain data presents an abrupt change at this moment (these outlier data have been removed during processing).

Taking the specimens at T=25°C as an example, it can be seen from Fig. 7(a) that the strain for all in the two directions presents a similar nonlinear changing trend with the loading time. The S-strain and V-strain behave as the tensile deformation and compression deformation before disk sample failure, respectively. The strain values are kept low in the initial loading phase, then increasing non-linearly with loading time and reaching a peak value when the specimens arrive at the peak tensile strength. It also can be observed that the strain evolutions (both S-strain and V-strain) are significantly affected by the bedding orientation. The absolute values of S-strain and V-strain show a decreasing trend with increasing bedding orientation. The specimen at a=0° shows the maximum strain value, and the minimum occurs at a=90°. For the specimens after different heat treatments, similar variation features for the two direction strain can be found in Figs. 7(b)-(f). It indicates that both the S-strain and V-strain of bedded sandstone strongly depend on the layer orientations at different temperatures.

The evolution of S-strain and V-strain at failure with bedding orientation for all the temperatures is shown in Fig.8. As shown in Fig.8, for all the temperatures except 25°C and 200°C, the maximum S-strain value is observed at a=0°. At 25°C and 200°C, the maximum S-strain value occurs at a=30°. For all the temperatures except 200°C and 1000°C, the maximum absolute value of V-strain is recorded at a=0°. While at 200 °C and 1000°C, the 30° bedding orientation shows the maximum value. It can be concluded that the peak strain (absolute value) at failure decreases gradually with increasing bedding orientation for all the temperatures. Although in some cases, the maximum appears at a=30 °, the overall change trend is nearly similar for all various temperatures.

At lower bedding orientation, the bedding planes are under compression and the tensile strength is mainly dependent on the rock matrix; thus, the specimens can undergo relatively higher strain before failure. However, the tensile fractures can easily occur along the bedding planes for the specimens with higher bedding orientation when the specimens experience a relatively lower amount strain. Thus, the S-strain and V-strain for the specimens with lower bedding orientation are larger than the higher bedding orientation. After different high-temperature treatments, the bedding orientation still has a significant effect on the deformation properties.

Fig.9 shows the development of S-strain and V-strain at failure with temperature for all the bedding orientations. It should be noted that the temperature has a significant effect

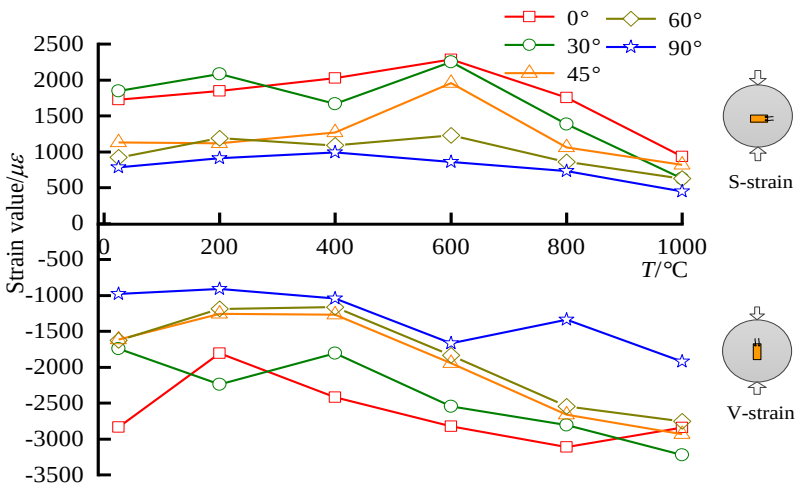

Fig. 9 Failure strain at different temperature for different bedding orientation

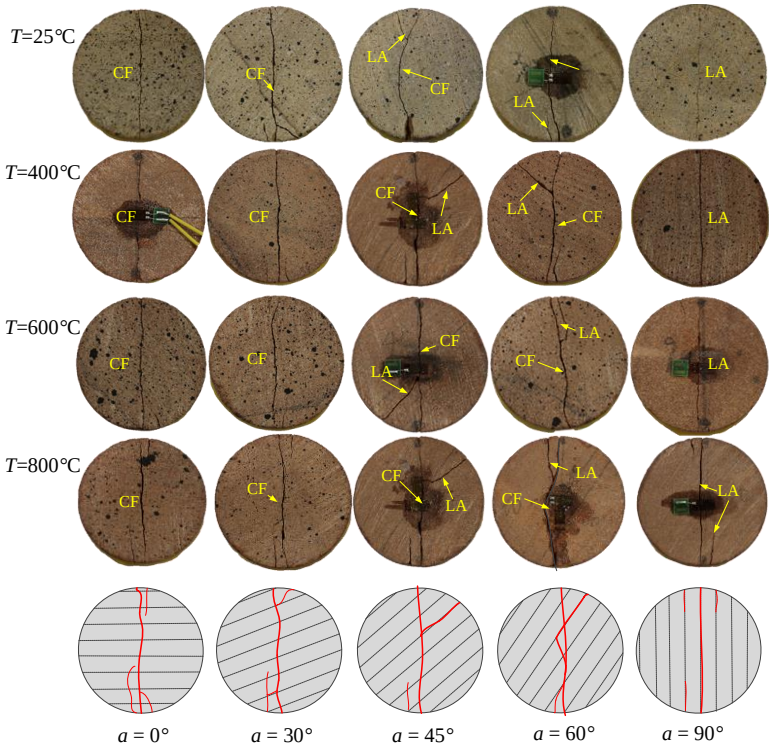

Fig. 10 Failure patterns of disk specimen with varying bedding orientation at different temperature

on the deformation properties of rock specimens for all bedding orientations. The S-strain increases first and then decreases with the increase of temperature. The maximum S-strain value usually occurs at 600°C except for the case of 90° bedding orientation, where the maximum is at 400°C. There are also some abnormal data in the figure. For example, at a=30°, the S-strain appears a slight fall in the range of 200°C ~ 400°C, which may be attributed to the single test data. It can also be seen intuitively that for the specimens with low bedding orientation (a=0°, 30° and 45°), the variation of S-strain is relatively rapid, but for the (a=60° and 90°), the variation is very gentle. This phenomenon indicates that the S-strain for the lower higher bedding orientation is more sensitive to temperature than the higher bedding orientation. Additionally, the S-strain evolution also confirms the mechanism of change of strength with temperature. Before 600°C, the high-temperature treatment increases the tensile deformation ability of the specimens, thus improving the tensile strength. As the temperature increases to the range of 800°C~ 1000°C, the tensile deformation is weakened, thus decreasing the tensile strength. However, for the V-strain, its absolute value shows an increasing trend with increasing temperature, which can be interpreted that the heat treatment increases the ductility and degrades the sandstone specimens' elastic modulus.

3.3 Failure patterns

Previous studies have proved that the failure patterns of

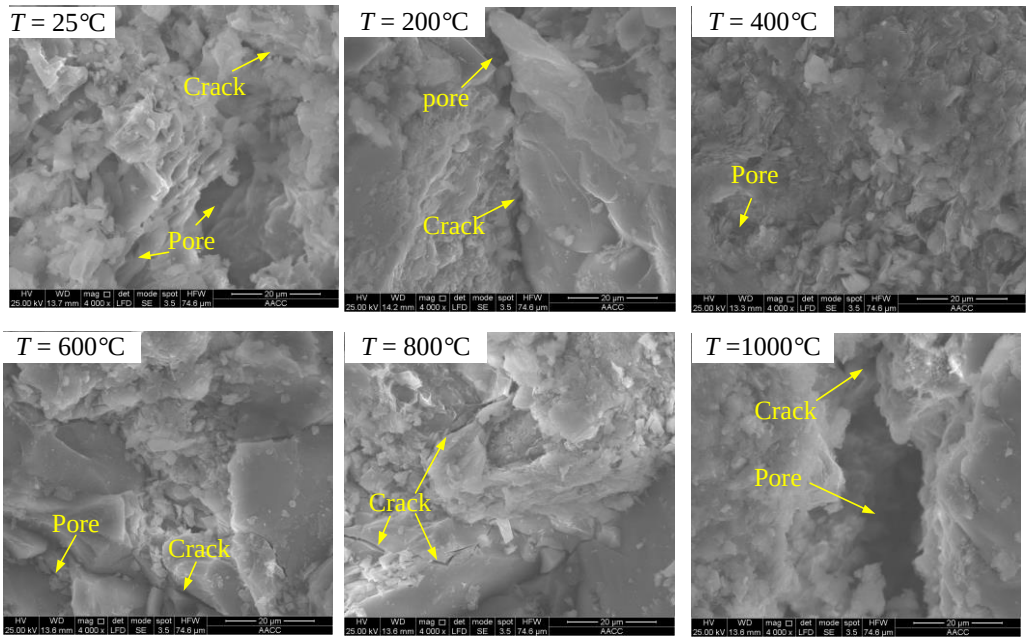

Fig. 11 SEM images of sandstone after different high-temperature treatment (×5000)

stratified isotropic rock are closely related to the bedding orientation. According to the classification methods introduced by Tavallali and Vervoort (2010), two types of failure fracture are observed in the broken disk specimens. One is the call "layer activation" (LA), whereby the fractures occur along the bedding planes; another is called "central fractures" (CF), whereby the fractures are roughly parallel to the loading direction and located in the central parts of the disk specimens. The observed failure patterns of disk specimens after failure are shown in Fig. 10. Considering the specimens with the same bedding orientation perform a similar failure pattern after different high-temperature treatment, here, we only display the typical failure specimens picture at T=25°C, 400°C, 600°C and 800°C.

For a=0° and 30°, CF-type fracture is the dominant failure mode. The predominant fracture passes through the bedding planes and is roughly parallel to the loading direction. Also, some secondary cracks usually occur at the end of the loading disk specimens. For a=45° and 60°, the failure specimens appear the combination of CF-type and LA-type failure mode. Apart from the predominant tensile fracture across the lamination (CF), an apparent shear fracture along the lamination can also be observed in the failed disk specimens. For a=90°, the failure specimens present a pure LA-type fracture mode, which is a straight fracture along the bedding plane.

The failure patterns of the specimens with a bedding orientation of 0° and 90° look similar. However, for a=90°, the predominant fracture is the tensile crack along the lamination, and the tensile crack is thinner and more upright. As previously mentioned failure pattern for a=0° is the tensile crack parallel to the loading direction (perpendicular to the bedding orientation), which should perform similar tensile properties to the "intact" rock. Nevertheless, for a=90°, the tensile strength of the disk specimen should rather correspond to the tensile strength of the weak "lamination". Thus, the tensile strength for a=90° is obviously smaller than that of a=0°, as shown in Fig. 3. It also can be seen that the LA-type fractures begin to occur at 45° and 60° bedding orientation, which can weaken the tensile strength of disk specimens partly compare with the 0° and 30° bedding orientation. The above failure patterns for different bedding orientations can further explain the conclusion that the tensile strength decreases with increasing bedding orientation.

It also should be noted that the high temperature does not have much effect on the failure mode of disk specimens of the bedded sandstone. The failure disk specimens appear similar failure features for the same bedding orientation at different temperatures. Thus, to better understand the mechanism of high temperature on tensile properties of bedded sandstone, the scanning electron microscope (SEM) analysis was carried out for different heat treatment specimens in the next section.

4. SEM analysis

Previous studies have demonstrated that the internal structure of rock materials changes dramatically as the heat-treatment temperature increases, resulting in significant changes in macroscopic parameters. SEM is a commonly used method to observe the internal structure of the rock specimens after being heated to different temperatures, which is effective for the study of the evolution of internal structure and proves the relevant experimental results. The SEM images of the grain structures and micro-fractures of the thermally treated sandstone specimens at a magnification of ×1000 are shown in Fig. 11.

At low temperature (below 200°C), the are some original pores and cracks are on the specimen profile. As the temperature increases to 400°C, the specimen profile looks smoother and denser and few defects (pores and

cracks) can be observed, which may contribute to the thermal expansion of the internal mineral particles causing the closure of the original cracks and pores. When the temperature reaches 600°C, some newly cracks between along mineral grains induced by thermal stress can be observed on the surface. As the temperature increases from 600°C to 800°C, the thermal stress became markedly enhanced, large amounts of transgranular cracks formed within the specimen. With a further increase in temperature to 1000°C, the original defects (pores and cracks) and newly cracks extend, widen, and penetrate each other, leading to further deterioration of the mechanical properties of sandstone.

Based on the above analysis, we can get the following conclusions: In the temperature range of 25 °C~600 °C, the thermal expansion of the internal mineral particles increases the compactness of rock with the increase of temperature, and the bond between the mineral grains are strengthened, thus increasing the mechanical properties of the sandstone specimens. As a result, the tensile strength, S-strain, and V-strain appear an increasing trend with the increasing temperature. However, after a higher temperature treatment of 800°C and 1000°C, the internal structure of the specimen is sharply deteriorated by thermal reactions, which significantly weakened the tensile properties of the specimens. Thus, the tensile strength and the tensile strain (S-strain) present a declining trend as the temperature increases from 600°C to 1000°C. On the other hand, the ductile of specimens is also improved after heat treatment, leading to the V-strain increasing with increasing temperature.

5. Conclusions

In this paper, a series of Brazilian tests were performed on the disk specimens of bedded sandstone with different bedding orientations after different high-temperature treatment. It is verified that the tensile properties and failure patterns are considerably affected by the bedding orientation and temperature. Based on the experimental results, the conclusions can be summarized as follows:

• The tensile strength exhibits a similar negative linear change with increasing bedding orientation at different temperatures. The maximum value usually occurs at α=0°, and the minimum value usually occurs at α=90°, which indicate the bedded sandstone possesses prominent anisotropy in tensile strength after different heat-treatment. The tensile strength is also significantly affected by the temperature, appearing the first increase and then decrease with increasing temperature for the same bedding orientation. The increasing temperature has more effect on the evolution of the tensile strength for low bedding orientation (α=0°) than the high bedding orientation (α=90°), which leads to the anisotropy coefficient first increase and then decrease with increasing temperature.

• The rock bedding orientation also profoundly affects the central strain of the disk specimens at different temperatures. The absolute values of the strain appear a gradually decreasing trend with increasing bedding orientation. The maximum V-strain and S-strain usually occur at α = 0° or 30°, and reduce to the minimum at α = 90°. For all bedding orientations, the S-strain first increases and then decreases, but V-strain keeps increasing with increasing temperature.

• Along with that, the bedding orientation also controls the failure patterns of the failed disk specimens. The failure patterns of the failed specimens are divided into three types, e.g., central across the bedding planes (CF), fracture along the bedding planes (LA) and the mixed fracture patterns of the two. The failure patterns change from a CF-type fracture at lower bedding orientation (α=0° and 30°) to a pure LA-type fracture at α=90°. At α=45° and 60°, the failed specimens appear a mixed failure pattern of CF-type and LA-type fractures.

Acknowledgments

This work is financially supported by National Natural Science Foundation of China (No52074259, 51734009).We also would like to express our sincere gratitude to the editor and reviewers for their valuable comments which have greatly improved this paper.

References

ASTM D3967–08, (2008), Standard test method for splitting tensile strength on intact rock core specimens, ASTM International, West Conshohocken, Pennsylvania, U.S.A.

Becattini, V., Motmans, T., Zappone, A., Madonna, C., Haselbacher, A. and Steinfeld, A. (2017), "Experimental investigation of the thermal and mechanical stability of rocks for high-temperature thermal-energy storage", *Appl. Energy*, **203**, 373-389. https://doi.org/10.1016/j.apenergy.2017.06.025.

Chen, G., Li, T., Wang, W., Guo, F. and Yin, H. (2017), "Characterization of the brittleness of hard rock at different temperatures using uniaxial compression tests", *Geomech. Eng.*, **13**(1), 63-77. https://doi.org/10.12989/gae.2017.13.1.063.

Cheng, Z.B., Li, L.H. and Zhang, Y.N. (2019), "Laboratory investigation of the mechanical properties of coal-rock combined body", *B. Eng. Geol. Environ.*, **79**(4), 1947-1958. https://doi.org/ 10.1007/s10064-019-01613-z.

Chong, Z.H., Li, X., Hou, P., Wu, Y., Zhang, J., Chen, T. and Liang, S. (2017), "Numerical investigation of bedding plane parameters of transversely isotropic shale", *Rock Mech. Rock Eng.*, **50**(5), 1-22. https://doi.org/10.1007/s00603-016-1159-x.

Debecker, B. and Vervoort, A. (2009), "Experimental observation of fracture patterns in layered slate", *Int. J. Fract.*, **159**, 51-62. https://doi.org/10.1007/s10704-009-9382-z.

Gholami, R. and Rasouli, V. (2014), "Mechanical and elastic properties of transversely isotropic slate", *Rock Mech. Rock Eng.*, **47**(5), 1763-1773. https://doi.org/10.1007/s00603-013-0488-2.

Keneti, A. and Wong, R. (2010), "Investigation of anisotropic behavior of Montney shale under indirect tensile strength test", *Proceedings of the Canadian Unconventional Resources and International Petroleum Conference*, Alberta, Canada, October.

Khanlari, G., Rafiei, B. and Abdilor, Y. (2015), "An experimental investigation of the Brazilian tensile strength and failure patterns of laminated sandstones", *Rock Mech. Rock Eng.*, **48**(2), 843-852. https://doi.org/10.1007/s00603-014-0576-y.

Komurlu, E., Kesimal, A. and Demir, S. (2016), "Experimental and numerical analyses on determination of indirect (splitting) tensile strength of cemented paste backfill materials under

different loading apparatus", *Geomech. Eng.*, **10**(6), 775-791. http://doi.org/10.12989/gae.2016.10.6.775.

Liu, X.S., Fan, D.Y., Tan, Y.L., Ning, J.G., Song, S.L., Wang, H.L. and Li, X.B. (2021), "New detecting method on the connecting fractured zone above the coal face and a case study", *Rock Mech. Rock Eng.*, 1-13. https://doi.org/10.1007/s00603-021-02487-y.

Lü, C., Sun, Q., Zhang, W.Q., Geng, J.S., Qi, Y.M. and Lu, L.L. (2017), "The effect of high temperature on tensile strength of sandstone", *Appl. Therm. Eng.*, **111**(25), 573-579. https://doi.org/10.1016/j.applthermaleng.2016.09.151.

Mokhtari, M., Bui, B.T., Tutuncu, A.N. (2014), "Tensile failure of shales: impacts of layering and natural fractures", *Proceedings of the SPE Western North American and Rocky Mountain Joint Meeting*, Denver, U.S.A., April.

Nasseri, M., Rao, K. and Ramamurthy, T. (2003), "Anisotropic strength and deformational behavior of Himalayan schists", *Int. J. Rock Mech. Min. Sci.*, **40**(1), 3-23. https://doi.org/10.1016/S1365-1609(02)00103-X.

Nezhad, M.M., Zhu, H.H., Woody Ju, J. and Chen, Q. (2016), "A simplified multiscale damage model for the transversely isotropic shale rocks under tensile loading", *Int. J. Damage Mech.*, **25**(5), 705-726. https://doi.org/10.1177/1056789516639531.

Roy, D.G. and Singh, T. (2016), "Effect of heat treatment and layer orientation on the tensile strength of a crystalline rock under Brazilian test condition", *Rock Mech. Rock Eng.*, **49**(5), 1663-1677. https://doi.org/10.1007/s00603-015-0891-y.

Sirdesai, N., Singh, T., Ranjith, P. and Singh, R. (2017), "Effect of varied durations of thermal treatment on the tensile strength of red sandstone", *Rock Mech. Rock Eng.*, **50**(1), 205-213. https://doi.org/10.1007/s00603-016-1047-4.

Tavallali, A. and Vervoort, A. (2010), "Effect of layer orientation on the failure of layered sandstone under Brazilian test conditions", *Int. J. Rock Mech. Min. Sci.*, **47**(2), 313-322. https://doi.org/10.1016/j.ijrmms.2010.01.001.

Tomac, I. and Sauter, M. (2018), "A review on challenges in the assessment of geomechanical rock performance for deep geothermal reservoir development", *Renew. Sust. Energy Rev.*, **82**, 3972-3980. https://doi.org/10.1016/j.rser.2017.10.076.

Wang, X., Yuan, W., Yan, Y. and Zhang, X. (2020), "Scale effect of mechanical properties of jointed rock mass: A numerical study based on particle flow code", *Geomech. Eng.*, **21**(3), 259-268. https://doi.org/10.12989/gae.2020.21.3.259.

Wang, J., Qiu, P.Q., Yang, S. and Shang, H.F. (2019), "Microseismic monitoring and its precursory parameter of hard roof collapse in longwall faces: A case study", *Geomech. Eng.*, **17**(4), 375-383. https://doi.org/ 10.12989/gae.2019.17.4.375.

Xue, Y.C., Sun, W.B. and Wu, Q. (2020), "The influence of magmatic rock thickness on fracture and instability law of mining surrounding rock", *Geomech. Eng.*, **20**(6), 547-556. https://doi.org/10.12989/gae.2020.20.6.000.

Yang, S.Q., Yin, P.F. and Huang, Y.H. (2019), "Experiment and discrete element modelling on strength, deformation and failure behaviour of shale under Brazilian compression", *Rock Mech. Rock Eng.*, **52**(11), 4339-4359. https://doi.org/10.1007/s00603-019-01847-z.

Yin, T.B., Li, X.B., Cao, W.Z. and Xia, K.W. (2015), "Effects of thermal treatment on tensile strength of Laurentian granite using Brazilian test", *Rock Mech. Rock Eng.*, **48**(6), 2213-2223. https://doi.org/10.1007/s00603-015-0712-3.

Zhou, Z.L., Cai, X., Ma, D., Chen, L., Wang, S.F. and Tan, L.H. (2018), "Dynamic tensile properties of sandstone subjected to wetting and drying cycles", *Constr. Build. Mater.*, **182**, 215-232. https://doi.org/10.1016/j.conbuildmat.2018.06.056.